

# Soluble Nylon-Functionalized Carbon Nanotubes from Anionic Ring-Opening Polymerization from Nanotube Surface

Liangwei Qu,<sup>†</sup> L. Monica Veca,<sup>†</sup> Yi Lin,<sup>†</sup>  
 Alex Kitaygorodskiy,<sup>†</sup> Bailin Chen,<sup>†</sup>  
 Alecia M. McCall,<sup>†</sup> John W. Connell,<sup>‡</sup> and  
 Ya-Ping Sun<sup>\*,†</sup>

Department of Chemistry and Laboratory for Emerging Materials and Technology, Clemson University, Clemson, South Carolina 29634-0973, and Advanced Materials and Processing Branch, NASA Langley Research Center, Mail Stop 226, Hampton, Virginia 23681-2199

Received August 8, 2005

Revised Manuscript Received October 4, 2005

## Introduction

The preparation of polymeric nanocomposites filled with single-walled carbon nanotubes (SWNTs) generally requires the nanotubes being homogeneously dispersed and compatible with the polymer matrix.<sup>1–3</sup> An effective approach for these requirements is to functionalize the nanotubes with polymers that are identical or structurally similar to the matrix polymers.<sup>4</sup> Among the widely pursued functionalization strategies is the “grafting-from” method, in which monomers or initiators are first attached to the nanotubes to serve as starting points for propagation.<sup>5–9</sup> The grafting-from strategy is generally similar to in situ polymerization,<sup>10</sup> but in a more controlled fashion. For example, the nanotube-bound radical initiators were used in the atom transfer radical polymerization to yield poly(methyl methacrylate)-, poly(*n*-butyl methacrylate)-, or poly(*tert*-butyl acrylate)-functionalized carbon nanotubes.<sup>5</sup>

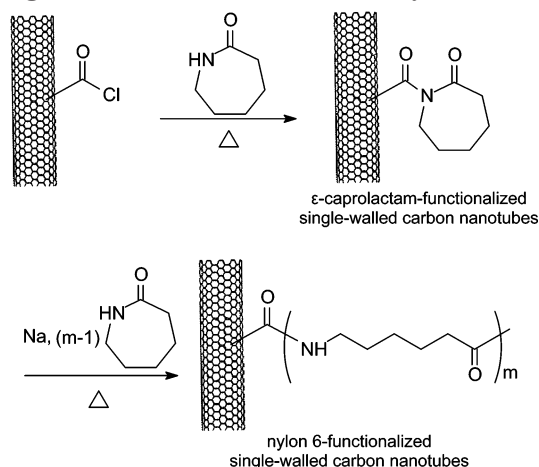
Nylon is an important commodity polymer with a wide variety of applications, and naturally, there has been much interest in nanocomposites of nylon with carbon nanotubes.<sup>11–16</sup> For the investigation of these materials, the preparation of nylon-functionalized carbon nanotubes is highly relevant and beneficial. In a typical synthesis of nylon-6,  $\epsilon$ -caprolactam is used as monomer in the efficient anhydrous polymerization with a base (anionic) as initiator.<sup>17</sup> In addition, the secondary amine in  $\epsilon$ -caprolactam may be used to form an amide linkage with the defect-derived carboxylic acid moiety on the carbon nanotube surface. We report here that the covalent attachment of  $\epsilon$ -caprolactam molecules to SWNTs could be the first step in a two-step grafting-from process of functionalizing the nanotubes with nylon-6. The second step was the anionic ring-opening polymerization of the nanotube-bound  $\epsilon$ -caprolactam species with the same monomers in bulk (Scheme 1).<sup>18</sup>

## Experimental Section

**Materials.**  $\epsilon$ -Caprolactam was purchased from Aldrich. Thionyl chloride and sodium were obtained from Alfa Aesar. Deuterated solvents for NMR measurements were supplied by Cambridge Isotope Laboratories.

The sample of SWNTs (arc-discharge method) was supplied by Carbon Solutions, Inc. It was purified by using a combination of thermal oxidation and oxidative acid treatment. In a

Scheme 1. Synthesis of Nylon-6-Functionalized Single-Walled Carbon Nanotubes (Nylon-SWNT)



typical experiment, a nanotube sample (1 g) was thermally oxidized in air in a furnace at 300 °C for 30 min. After the thermal treatment, the remaining sample was added to an aqueous HNO<sub>3</sub> solution (2.6 M), and the mixture was refluxed for 24 h. Upon centrifuging at 1000g to discard the supernatant, the remaining solids were washed with deionized water until neutral pH and then dried under vacuum.

**Measurements.** NMR measurements were performed on a JEOL Eclipse +500 NMR spectrometer and a Bruker Avance 500 spectrometer that is equipped with a high-resolution magic-angle-spinning (HR-MAS) probe designed specifically for gel-phase NMR. Optical absorption spectra were recorded on a Shimadzu UV3100 spectrophotometer. Raman spectra were obtained on a Renishaw Raman spectrometer equipped with a 50 mW diode laser source for 785 nm excitation and a CCD detector. Thermogravimetric analysis (TGA) was carried out on a Mettler-Toledo TGA/SDTA851e system. Scanning electron microscopy (SEM) images were obtained on a Hitachi S4700 field-emission SEM system. Atomic force microscopy (AFM) analysis was conducted on a Molecular Imaging PicoPlus system equipped with a multipurpose scanner. The height profile analyses were assisted by using the SPIP software distributed by Image Metrology.

**Caprolactam-SWNT.** A purified SWNT sample (50 mg) was mixed with thionyl chloride (10 mL), and the mixture was stirred and refluxed (70 °C) for 24 h. Upon removal of excess thionyl chloride under vacuum,  $\epsilon$ -caprolactam (5 g, 44 mmol) was added. The mixture was stirred at 110 °C for 24 h and then cooled to room temperature. Chloroform (20 mL) was added to the mixture, and the resulting suspension was filtered (0.22  $\mu$ m PVDF membrane). The solid sample from the filtration was extracted with chloroform for 6 h in a Soxhlet extractor to remove any residual  $\epsilon$ -caprolactam. Upon drying in a vacuum at room temperature, the  $\epsilon$ -caprolactam-functionalized SWNTs (caprolactam-SWNT) were obtained as a dark-colored powdery sample.

**Nylon-SWNT.** A caprolactam-SWNT sample (50 mg) was mixed with  $\epsilon$ -caprolactam (10 g, 88 mmol), and sodium (40 mg, 1.7 mmol) was added to the mixture as initiator for the polymerization reaction at 140 °C under nitrogen protection for 24 h (Scheme 1). The reaction mixture was dissolved in formic acid (10 mL), precipitated into water (50 mL), and filtered (0.22  $\mu$ m PVDF membrane). The resulting solid sample was washed successively (25 mL each) with formic acid, water, and formic acid again to remove sodium salts and those polymers not attached to the nanotubes (until no such polymers found in the filtrate). The cleaned sample was dispersed in formic acid (10 mL), followed by centrifuging (3000g) to retain the dark-colored supernatant. The solvent formic acid

<sup>†</sup> Clemson University.

<sup>‡</sup> NASA Langley Research Center.

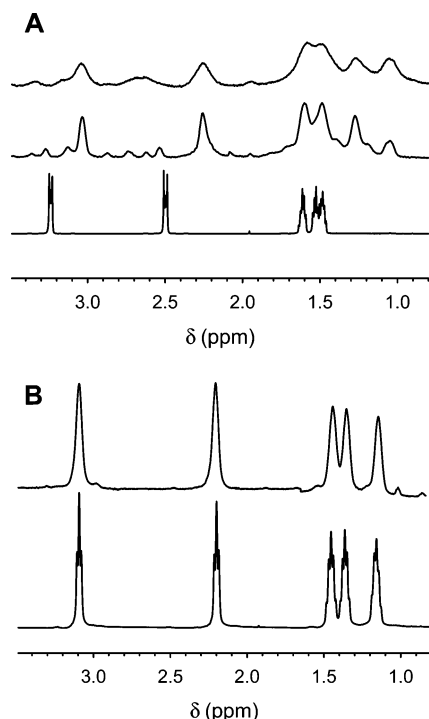


**Figure 1.** (A)  $^1\text{H}$  NMR spectra of  $\epsilon$ -caprolactam-functionalized single-walled carbon nanotubes (caprolactam-SWNT) dispersed in deuterated formic acid (top: measured in solution probe; middle: in high-resolution magic angle spinning probe) are compared with that of  $\epsilon$ -caprolactam (bottom). (B) A comparison of  $^1\text{H}$  NMR spectra of nylon-6-functionalized SWNTs (nylon-SWNT, top) and nylon-6 (bottom) in deuterated formic acid solutions.

was removed on a rotatory evaporator to yield nylon-6-functionalized SWNTs (nylon-SWNT) as black solids.

## Results and Discussion

The functionalization of SWNTs with  $\epsilon$ -caprolactam was the first step in the grafting-from process. The caprolactam-SWNT sample was generally insoluble in common organic solvents. Nevertheless, its dispersion in formic acid was used for  $^1\text{H}$  NMR measurement, yielding rather broad resonances (Figure 1). The broadening was probably due in part to the heterogeneous nature of the dispersion, in addition to the high molecular weight and low mobility of carbon nanotubes. Better resolved proton signals were obtained from the same dispersion by using a high-resolution magic-angle-spinning (HR-MAS) probe designed specifically for gel-phase NMR (Figure 1). The resonances of the nanotube-attached  $\epsilon$ -caprolactam were systematically shifted upfield from those of the starting  $\epsilon$ -caprolactam, especially for the methylene protons near the expected amide linkage (3.24 and 2.50 ppm vs 3.03 and 2.25 ppm, Figure 1). In the literature,<sup>20,21</sup> similar upfield shifts have been attributed to effects associated with the large aromatic ring current in nanotubes, which are more pronounced when the protons are closer to the nanotube surface. The NMR results are consistent with the covalent attachment of  $\epsilon$ -caprolactam molecules to SWNTs.

The FT-IR spectrum of the caprolactam-SWNT sample exhibited absorptions at 2930 and 2860  $\text{cm}^{-1}$ , corresponding to the stretching modes of alkyl C-H in  $\epsilon$ -caprolactam. As compared in Figure 2, the Raman spectrum (785 nm excitation) of the caprolactam-SWNT sample is similar to that of purified SWNTs, showing typical radial breathing mode (170  $\text{cm}^{-1}$ ),

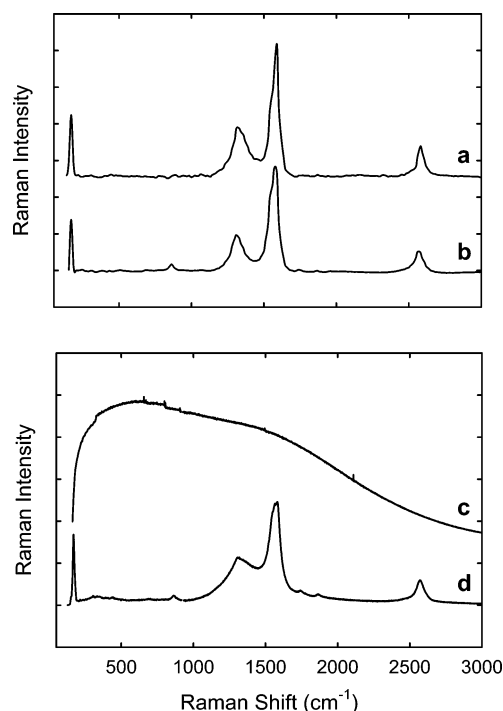


**Figure 2.** Raman spectra (785 nm excitation) of the purified single-walled carbon nanotube (SWNT) sample (a), caprolactam-SWNT (b), and nylon-6-functionalized SWNTs (nylon-SWNT) before (c) and after (d) thermal defunctionalization (800  $^{\circ}\text{C}$ ,  $\text{N}_2$ ).

D-band (1310  $\text{cm}^{-1}$ ), tangential G-band (1580  $\text{cm}^{-1}$ ), and D\*-band (2660  $\text{cm}^{-1}$ ) features. The absence of luminescence interference reflects the expected low functional group content in the caprolactam-SWNT sample, also consistent with the poor solubility of the sample. In thermogravimetric analysis (TGA) of the sample under inert atmosphere, the covalently attached  $\epsilon$ -caprolactam on the nanotube surface could be selectively removed (or "thermal defunctionalization"),<sup>1,4,6-8</sup> which allowed an estimate of the  $\epsilon$ -caprolactam content in the sample. The content was indeed low,  $\sim 7\%$  (w/w), as expected. It corresponds to on average one  $\epsilon$ -caprolactam for every 125 nanotube carbons.

The second step in the grafting-from process was the sodium-initiated anionic ring-opening polymerization to obtain nylon-6-functionalized SWNTs. The final nylon-SWNT sample contained more than 70% of the starting SWNTs. The sample was soluble in some organic solvents, such as formic acid and *m*-cresol, resulting in dark-colored but optically transparent solutions.

The  $^1\text{H}$  NMR spectrum of nylon-SWNT in deuterated formic acid is compared with that of commercially available nylon-6 (Acros,  $M_n \sim 10\,000$ ) in Figure 1. The chemical shifts in the two spectra are generally similar, but the resonances of the nanotube-bound nylon moieties are obviously broader. Unlike in the dispersion of caprolactam-SWNT discussed above, the broadening here is probably due entirely to the nylon species being associated with the nanotubes (high molecular weight and low mobility) because the nylon-SWNT solution is homogeneous.

The nylon functionalities on the nanotube surface could also be selectively removed in TGA under an inert atmosphere (thermally defunctionalized), similarly allowing an estimate of the nanotube content. According to the amount of residue at 500  $^{\circ}\text{C}$ , the nylon-SWNT sample contained about 40% (w/w) of nanotubes.<sup>22</sup>

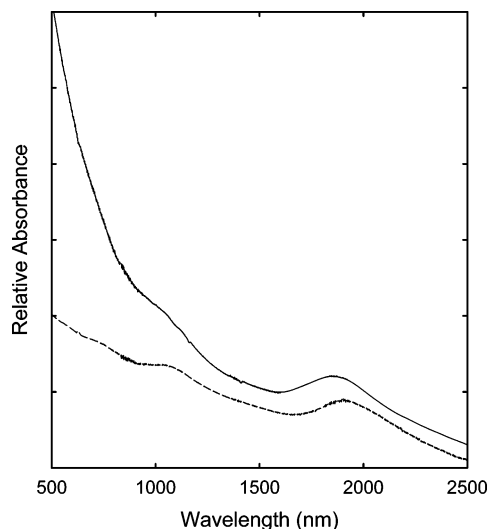


**Figure 3.** Absorption spectra of nylon-6-functionalized single-walled carbon nanotubes (nylon-SWNT, top) and the purified SWNT sample (bottom) on glass substrate.

The optical absorption spectrum of nylon-SWNT is shown in Figure 3. The broad  $S_{11}$  and  $S_{22}$  bands at 1870 and 1050 nm, respectively, are characteristic of the electronic transitions associated with the van Hove singularity pairs in semiconducting SWNTs.<sup>23</sup> The spectral similarity to that of purified SWNTs suggests that neither the polymerization reaction nor the presence of nylon functionalities on the nanotube surface changes in any substantial fashion the electronic transitions. Apparently, the nanotube electronic structures are largely preserved in the nylon-functionalized SWNTs, as also found in a number of other functionalizations that target the nanotube surface defect-derived carboxylic acids.<sup>4,7</sup>

The Raman characterization of nylon-SWNT was hindered by overwhelming luminescence interference, quite different from the same characterization of the precursor caprolactam-SWNT (Figure 2). As reported recently,<sup>24</sup> the substantial difference in the extent of luminescence interference in Raman measurements is an indication on how well the nanotubes are dispersed and functionalized. In the nylon-SWNT sample, soluble in selected solvents to form transparent solutions, the nanotubes were well-dispersed, and their surface defects were likely passivated as a result of the effective functionalization, thus corresponding to stronger nanotube defect-derived luminescence.<sup>1,24</sup> The thermal defunctionalization obviously "undispersed" the nanotubes, suppressing or completely eliminating the luminescence interference. As compared in Figure 2, the Raman spectrum of the thermally defunctionalized nylon-SWNT sample again exhibits features similar to those of purified SWNTs.

A direct SEM imaging of the nylon-functionalized SWNTs was somewhat difficult because of a significant amount of soft (nylon polymer) materials in the specimen (Figure 4). However, the removal of nylon via thermal defunctionalization obviously made the SEM analysis more straightforward, with the resulting image showing abundant SWNTs (Figure 4). AFM is applicable to the direct analysis of functionalized carbon nanotubes. For nylon-SWNT, the specimen for AFM analysis was prepared by spraying a dilute formic acid solution of the sample onto a mica substrate. During the spraying, the substrate was kept at 120 °C to

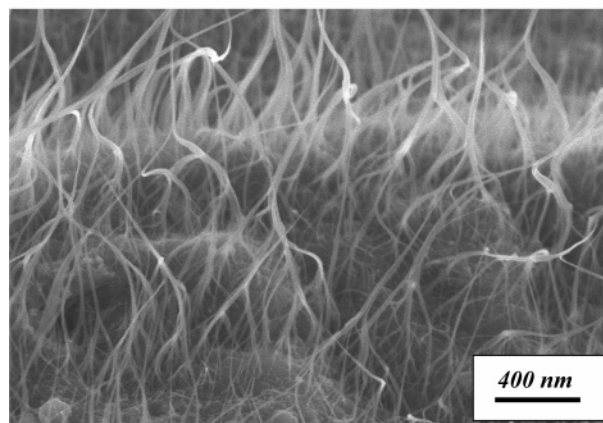
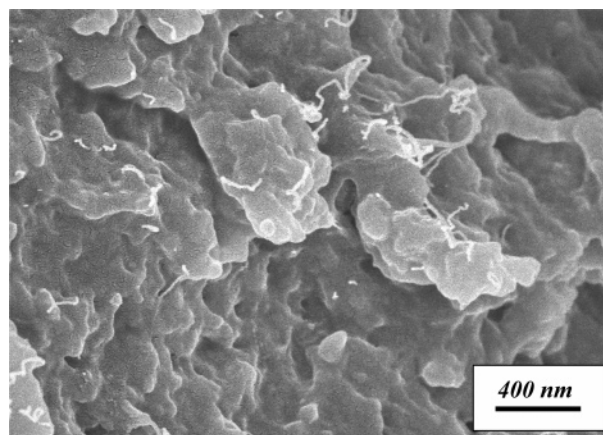


**Figure 4.** Scanning electron microscopy (SEM) images of the nylon-6-functionalized single-walled carbon nanotubes (nylon-SWNT) sample before (top) and after (bottom) thermal defunctionalization (800 °C,  $N_2$ ).

facilitate rapid solvent evaporation in an effort to preserve the original nanotube dispersion in the solution. A representative AFM topographic image from the analysis of such a specimen is shown in Figure 5. There are apparently abundant nanotubes of different lengths (hundreds of nanometers), mostly well-dispersed to the individual nanotube level according to the height analysis (Figure 5). It seems that the AFM specimen was unusually well-prepared (with a significant population of well-dispersed individual SWNTs), which probably benefitted from the use of the highly polar solvent formic acid. The solvent effect might be that the nanotube surface is charged, as in the superacid dispersion<sup>25</sup> or electrolyte-assisted dispersion of carbon nanotubes,<sup>26</sup> thus resulting in more efficient exfoliation of the nanotube bundles (or preventing the functionalized SWNTs from aggregating).

In summary, the functionalization of SWNTs with nylon-6 was accomplished by using the grafting-from strategy in a two-step process, where the covalent attachment of  $\epsilon$ -caprolactam molecules to nanotubes was followed by the anionic ring-opening polymerization of these bound  $\epsilon$ -caprolactam species with the same monomers in bulk. The resulting sample was characterized systematically, and the results were supportive of the expected covalent functionalization of SWNTs by nylon-6. This is a relatively convenient but still reasonably controllable method to chemically modify carbon nanotubes with a commodity polymer of extremely wide uses. The solubility of the functionalized nanotube sample in some organic solvents may prove valuable to



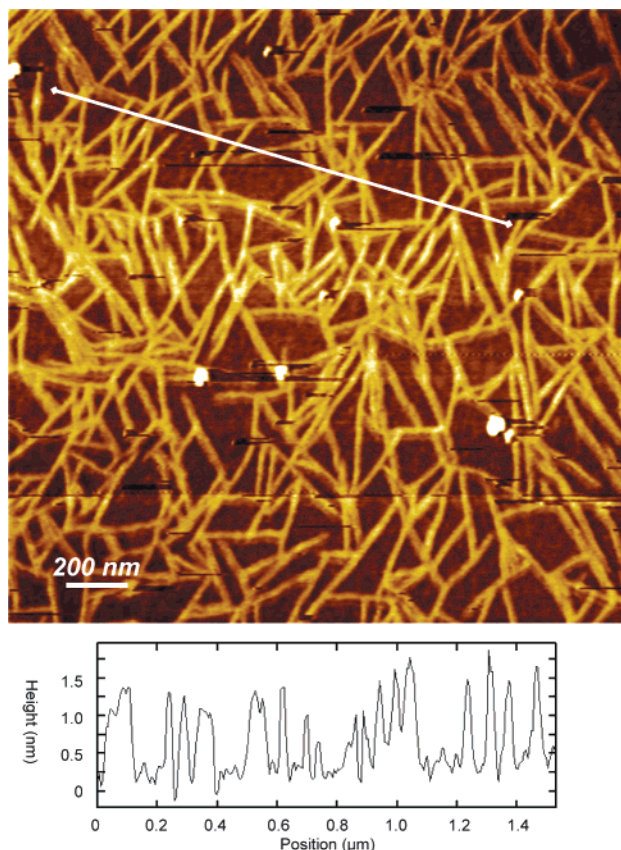


**Figure 5.** Atomic force microscopy (AFM) topography image (top) and height analysis (bottom) of a nylon-6-functionalized single-walled carbon nanotubes (nylon-SWNT) specimen (prepared by spraying the sample solution onto a heated mica substrate).

the homogeneous dispersion of SWNTs in nylon for high-quality nanocomposite materials.

**Acknowledgment.** We thank K. A. S. Fernando and B. Zhou for experimental assistance. Financial support from NASA and NSF is gratefully acknowledged. A.M. was a participant of the Summer Undergraduate Research Program sponsored jointly by NSF and Clemson University.

## References and Notes

- Sun, Y.-P.; Fu, K.; Lin, Y.; Huang, W. *Acc. Chem. Res.* **2002**, *35*, 1096–1104.
- Grady, B. P.; Pompeo, F.; Shambaugh, R. L.; Resasco, D. E. *J. Phys. Chem. B* **2002**, *106*, 5852–5858.
- Mitchell, C. A.; Bahr, J. L.; Arepalli, S.; Tour, J. M.; Krishnamoorti, R. *Macromolecules* **2002**, *35*, 8825–8830.
- (a) Hill, D. E.; Lin, Y.; Rao, A. M.; Allard, L. F.; Sun, Y.-P. *Macromolecules* **2003**, *35*, 9466–9471. (b) Lin, Y.; Zhou, B.; Fernando, K. A. S.; Liu, P.; Allard, L. F.; Sun, Y.-P. *Macromolecules* **2003**, *36*, 7199–7204. (c) Qu, L.; Lin, Y.; Hill, D. E.; Zhou, B.; Wang, W.; Sun, X.; Kitaygorodskiy, A.; Suarez, M.; Connell, J. W.; Allard, L. F.; Sun, Y.-P. *Macromolecules* **2004**, *37*, 6055–6060.
- (a) Yao, Z.; Braid, N.; Botton, G. A.; Adronov, A. *J. Am. Chem. Soc.* **2003**, *125*, 16015–16024. (b) Kong, H.; Gao, C.; Yan, D. *J. Am. Chem. Soc.* **2004**, *126*, 412–413. (c) Qin, S.; Qin, D.; Ford, W. T.; Resasco, D. E.; Herrera, J. E. *J. Am. Chem. Soc.* **2004**, *126*, 170–176. (d) Baskaran, D.; Mays, J. W.; Bratcher, M. S. *Angew. Chem., Int. Ed.* **2004**, *43*, 2138–2142.
- Liu, Y.; Adronov, A. *Macromolecules* **2004**, *37*, 4755–4760.
- (a) Kong, H.; Li, W.; Gao, C.; Yan, D.; Jin, Y.; Walton, D. R. M.; Kroto, H. W. *Macromolecules* **2004**, *37*, 6683–6686. (b) Xu, Y.; Gao, C.; Kong, H.; Yan, D.; Jin, Y. Z.; Watts, P. C. P. *Macromolecules* **2004**, *37*, 8846–8853. (c) Gao, C.; Jin, Y. Z.; Kong, H.; Whitby, R. L. D.; Acquah, S. F. A.; Chen, G. Y.; Qian, H.; Hartschuh, A.; Silva, S. R. P.; Henley, S.; Fearon, P.; Kroto, H. W.; Walton, D. R. M. *J. Phys. Chem. B* **2005**, *109*, 11925–11932.
- (8) Qin, S.; Qin, D.; Ford, W. T.; Resasco, D. E.; Herrera, J. E. *Macromolecules* **2004**, *37*, 752–757.
- (9) (a) Hong, C.-Y.; You, Y.-Z.; Wu, D.; Liu, Y.; Pan, C.-Y. *Macromolecules* **2005**, *38*, 2606–2611. (b) Hong, C.-Y.; You, Y.-Z.; Pan, C.-Y. *Chem. Mater.* **2005**, *17*, 2247–2254.
- Tang, B. Z.; Xu, H. *Macromolecules* **1999**, *32*, 2569–2576.
- Stevens, J. L.; Huang, A. Y.; Peng, H.; Chiang, I. W.; Khabashesku, V. N.; Margrave, J. L. *Nano Lett.* **2003**, *3*, 331–336.
- Xia, H.; Wang, Q.; Qiu, G. *Chem. Mater.* **2003**, *15*, 3879–3886.
- (13) (a) Zhang, W. D.; Shen, L.; Phang, I. Y.; Liu, T. *Macromolecules* **2004**, *37*, 256–259. (b) Liu, T.; Phang, I. Y.; Shen, L.; Chow, S. Y.; Zhang, W.-D. *Macromolecules* **2004**, *37*, 7214–7222.
- Sandler, J. K. W.; Pegel, S.; Cadek, M.; Gojny, F.; van Es, M.; Lohmar, J.; Blau, W. J.; Schulte, K.; Windle, A. H.; Shaffer, M. S. P. *Polymer* **2004**, *45*, 2001–2015.
- Li, C. Y.; Li, L.; Cai, W.; Kodjie, S. L.; Tenneti, K. K. *Adv. Mater.* **2005**, *17*, 1198–1202.
- Endo, M.; Koyama, S.; Matsuda, Y.; Hayashi, T.; Kim, Y.-A. *Nano Lett.* **2005**, *5*, 101–105.
- Aharoni, S. M. *n-Nylons: Their Synthesis, Structure and Properties*; John Wiley & Sons: Chichester, 1997.
- During our investigation, Haddon and co-workers reported a scheme for preparing nanocomposites of nylon-6 with SWNTs, in which nitric acid-treated SWNTs were mixed with  $\epsilon$ -caprolactam for in situ cationic ring-opening polymerization.<sup>19</sup>
- Gao, J.; Itkis, M. E.; Yu, A.; Bekyarova, E.; Zhao, B.; Haddon, R. C. *J. Am. Chem. Soc.* **2005**, *127*, 3847–3854.
- (20) (a) Chen, J.; Liu, H.; Weimer, W. A.; Halls, M. D.; Waldeck, D. H.; Walker, G. C. *J. Am. Chem. Soc.* **2002**, *124*, 9034–9035. (b) Holzinger, M.; Abraham, J.; Whelan, P.; Graupner, R.; Ley, L.; Hennrich, F.; Kappes, M.; Hirsch, A. *J. Am. Chem. Soc.* **2003**, *125*, 8566–8580. (c) Ruther, M. G.; Frehill, F.; O'Brien, J. E.; Minett, A. I.; Blau, W. J.; Vos, J. G.; in het Panhuis, M. *J. Phys. Chem. B* **2004**, *108*, 9665–9668.
- According to the software ACD/HNMR Predictor for predicting NMR chemical shifts, amidation should result in downfield shifts of as much as 0.5–1 ppm for the adjacent caprolactam methylene protons. Therefore, the observed upfield shifts must be due to strong influence of the nanotube aromatic system, which overcomes the opposite effect from the amidation.
- Based on the population of  $\epsilon$ -caprolactam in the caprolactam-SWNT sample, the composition in nylon-SWNT corresponds to about 20 repeating units in each nanotube-attached nylon-6 chain (molecular weight  $\sim$  2200).
- Niyogi, S.; Hamon, M. A.; Hu, H.; Zhao, B.; Bhowmik, P.; Sen, R.; Itkis, M. E.; Haddon, R. C. *Acc. Chem. Res.* **2002**, *35*, 1105–1113.
- Lin, Y.; Zhou, B.; Martin, R. B.; Henbest, K. B.; Harruff, B. A.; Riggs, J. E.; Guo, Z.-X.; Allard, L. F.; Sun, Y.-P. *J. Phys. Chem. B* **2005**, *109*, 14779–14782.
- Davis, V. A.; Ericson, L. M.; Parra-Vasquez, A. N. G.; Fan, H.; Wang, Y.; Prieto, V.; Longoria, J. A.; Ramesh, S.; Saini, R. K.; Kittrell, C.; Billups, W. E.; Adams, W. W.; Hauge, R. H.; Smalley, R. E.; Pasquali, M. *Macromolecules* **2004**, *37*, 154–160.
- Penicaud, A.; Poulin, P.; Derre, A.; Anglaret, E.; Petit, P. *J. Am. Chem. Soc.* **2005**, *127*, 8–9.

MA051762N